Rank-Based Identification of High-dimensional Surrogate Markers: Application to Vaccinology

Arthur Hughes, Layla Parast, Rodolphe Thiébaut, Boris P. Hejblum

Rank-Based Identification of High-dimensional Surrogate Markers: Application to Vaccinology

Arthur Hughes[1,2], Layla Parast[3], Rodolphe Thiébaut[1,2,4], and Boris P. Hejblum[1,2]

[1]INSERM Bordeaux Population Health Research Center, INRIA SISTM, University of Bordeaux, F-33000 Bordeaux, France
[2]Vaccine Research Institute, F-94000 Créteil, France
[3]Department of Statistics and Data Science, University of Texas at Austin, Austin, TX 78712, United States of America
[4]Centre Hospitalier Universitaire de Bordeaux, Service d'Information Médicale, INSERM, Bordeaux F-33000, France

Abstract

In vaccine trials with long-term participant follow-up, it is of great importance to identify surrogate markers that accurately infer long-term immune responses. These markers offer practical advantages such as providing early, indirect evidence of vaccine efficacy, and can accelerate vaccine development while identifying potential biomarkers. High-throughput technologies like RNA-sequencing have emerged as promising tools for understanding complex biological systems and informing new treatment strategies. However, these data are high-dimensional, presenting unique statistical challenges for existing surrogate marker identification methods. We introduce Rank-based Identification of high-dimensional SurrogatE Markers (RISE), a novel approach designed for small sample, high-dimensional settings typical in modern vaccine experiments. RISE employs a non-parametric univariate test to screen variables for promising candidates, followed by surrogate evaluation on independent data. Our simulation studies demonstrate RISE's desirable properties, including type one error rate control and empirical power under various conditions. Applying RISE to a clinical trial for inactivated influenza vaccination, we sought to identify genes whose post-vaccination expression could serve as a surrogate for the induced immune response. This analysis revealed a signature of genes whose combined expression at 1 day post-injection appears to be a reasonable surrogate for the neutralising antibody titres at 28 days after vaccination. Pathways related to innate antiviral signalling and interferon stimulation were strongly represented in this derived surrogate, providing a clear immunological interpretation.

Keywords: Surrogate Marker, High-Dimensional, Non-parametric statistics, Transcriptomics, Vaccine

1 Introduction

The goal of a randomised clinical trial is typically to evaluate the efficacy of a treatment on a primary outcome. However, measuring this primary outcome can be time-consuming, costly, impractical, or unethical. Consequently, there is significant interest in identifying and validating surrogate markers that can accurately infer the treatment effect on the primary outcome without its direct observation [1].

The identification of surrogate markers is especially important in the context of vaccine clinical trials. In public health emergencies, such as the COVID-19 pandemic, validated surrogates enable accelerated vaccine development by providing evidence for candidate vaccine selection in early stage trials [2]. Furthermore, surrogate markers may allow for validation of new-generation vaccines where an efficacy trial would not be ethical, such as when a successful vaccine already exists, or when efficacy trials are not feasible in the absence of disease outbreak [3].

High-throughput technologies have emerged as promising candidates to better inform effective vaccine design [4]. A prime example is transcriptomic data, which describe gene expression – a dynamic process through which fixed information encoded in DNA is transformed into proteins which then in turn shape phenotypes. The gene expression response to vaccination is highly upstream, with changes observed in the first days following vaccination and mainly capturing innate responses [5]. Traditional immunological outcomes, however, such as antigen-specific antibody titres or T-cell responses, are fully established over weeks and months [6]. Therefore, a subset of genes whose expression serves as a surrogate for a vaccine's immunogenicity would have significant utility. For example, they could be invaluable in adaptive clinical trials that rely on rapidly measurable endpoints [7]. Additionally, studies have previously demonstrated that early gene expression measurements can predict individual immune responses to vaccination [8, 9, 10]. However, whether these gene expression markers (either individually or in combination) could serve as reliable surrogates for the vaccine response remains to be seen.

The statistical methods for evaluating surrogate markers have significantly evolved and improved over the past four decades. Prentice's landmark paper defined a surrogate marker as one that ensures that any test of the treatment's effect on the surrogate is also a valid test of its effect on the primary endpoint [11]. In the spirit of this definition, many papers have focused on developing methodologies to evaluate the proportion of the treatment effect on the primary outcome explained by the treatment effect on a surrogate marker (PTE) [12, 13, 14, 15, 16]. A surrogate may be validated for practical use if it captures some large, clinically relevant proportion of the treatment effect on the primary outcome. However, available methods typically require model specification; when the true model is unknown, the conclusions made about the surrogates may be invalid [13, 14, 15, 16, 13, 17, 18, 19]. In addition, such methods that require parametric assumptions are hard to verify in a small sample size setting. Moreover, the few non-parametric alternatives that are available rely on kernel smoothing, which performs poorly without a large sample [16, 20]. Thus, currently available methods are generally not well-equipped for the small sample size setting. Finally, surrogate evaluation is complicated in the multiple surrogate setting, especially when the dimension of the candidate surrogates is high. Some existing methods allow for the evaluation of the overall strength of a collection of candidate surrogates, for example by estimating their overall PTE, but do not offer a way to screen high-dimensional surrogates to identify a subset of markers which capture a large proportion of the treatment's effect on the response [20, 21, 22].

These limitations make existing methodology difficult to apply in practice to vaccine trials, where the model relating the primary outcome to the surrogates is complex and unknown, the sample size is typically small, and the candidate surrogates may be high-dimensional. Motivated by the application to vaccine development, we extend a recent approach by Parast *et al.* (2024) [22], which is a fully non-parametric rank-based approach, to the multiple marker setting. We propose *Rank-based Identification of high-dimensional SurrogatE markers* (RISE) – a two step approach, which first screens a set of high-dimensional variables, and then evaluates their overall strength as a surrogate. We apply this approach to a clinical trial for seasonal inactivated influenza vaccination, seeking to identify and evaluate potential gene expression surrogate markers of the vaccine immunogenicity.

2 Methods

2.1 Notation

Let n denote the total sample size, which is assumed to be small. Let Y denote the primary outcome, $A \in \{1, 0\}$ denote a binary vaccine indicator (e.g., vaccine or placebo), and $\boldsymbol{S} = (S_1, \ldots, S_p)$ denote a set of candidate surrogates, where we may have $p >> n$. Without loss of generality, we assume higher

values of Y and S_j are "better", with $j \in \{1, \ldots, p\}$. We adopt counterfactual notations, where each individual has a set of potential outcomes $\left[Y^1, Y^0, \boldsymbol{S}^1, \boldsymbol{S}^0\right]$. Here, Y^a and $\boldsymbol{S}^a$ represent the values of the primary outcome and surrogate markers, respectively, if the treatment had been, potentially counter to fact, set to $A = a$. The observed data consist of n_1 independent, identically distributed (i.i.d.) copies of $Y^1, \boldsymbol{S}^1$ for individuals in the treatment group and n_0 i.i.d. copies of $Y^0, \boldsymbol{S}^0$ for individuals in the control group, with $n = n_0 + n_1$.

2.2 Existing Rank-based Approach for a Single Surrogate

We first summarise a recently proposed approach by Parast *et al.* (2024) to evaluate a single surrogate in the small sample setting [22]. Motivated by Prentice's definition of a surrogate, this approach aims to identify a single surrogate S_j as valid if a test for a treatment effect based on the surrogate is a valid test for the treatment effect based on the primary outcome. Let

$$U_Y = \mathbb{P}(Y^1 > Y^0) + \frac{1}{2}\mathbb{P}(Y^1 = Y^0)$$

$$U_{S_j} = \mathbb{P}(S_j^1 > S_j^0) + \frac{1}{2}\mathbb{P}(S_j^1 = S_j^0),$$

where U_Y is simply a measure of the treatment effect on Y, and $U_Y \in (0.5, 1]$ indicates a positive treatment effect on Y, $U_Y \in [0, 0.5)$ indicates a negative effect on Y, and $U_Y = 0.5$ indicates no effect. Similarly, U_{S_j} quantifies the treatment effect on S_j. The general idea behind this approach is that the closer U_Y and U_{S_j} are to each other, the more S_j captures the treatment effect on Y and thus, is a stronger candidate surrogate marker for Y. The strength of the surrogate is quantified by the difference

$$\delta_j = U_Y - U_{S_j}$$

such that the closer δ_j is to 0, the stronger S_j is as a surrogate for Y. One could then consider S_j to be a valid surrogate if δ_j is bounded by some pre-specified upper bound ϵ. This is formalised through a non-inferiority test:

$$H_0 : \delta_j \geq \epsilon \quad \text{versus} \quad H_1 : \delta_j < \epsilon \tag{1}$$

where failure to reject H_0 reflects a poor surrogate, and rejection of H_0 reflects a valid surrogate. The quantities U_Y and U_{S_j} can be estimated as

$$\widehat{U}_Y = (n_1 n_0)^{-1} \sum_{i=1}^{n_1} \sum_{k=1}^{n_0} G(Y_{i1}, Y_{k0}) \qquad \text{and} \qquad \widehat{U}_{S_j} = (n_1 n_0)^{-1} \sum_{i=1}^{n_1} \sum_{k=1}^{n_0} G(S_{ji1}, S_{jk0})$$

where

$$G(A, B) = \begin{cases} 1, & \text{if} \quad A > B \\ \frac{1}{2}, & \text{if} \quad A = B \\ 0, & \text{if} \quad B < A \end{cases}$$

and Y_{ia} and S_{jia} denote the observed values of the primary response and j^{th} surrogate for individuals i such that $A_i = a$. Here, $\widehat{U}_Y$ is simply the rank-based Mann-Whitney U-statistic examining the difference in Y between the two groups and similarly for $\widehat{U}_{S_j}$, where $E(\widehat{U}_Y) = U_Y$ and $E(\widehat{U}_{S_j}) = U_{S_j}$ [23].

Then, for a given S_j, one can calculate $\widehat{\delta}_j = \widehat{U}_Y - \widehat{U}_{S_j}$. A closed-form expression for the standard deviation of $\widehat{\delta}_j$, denoted $\widehat{\sigma}_{\delta_j}$, is given in Parast *et al.* (2024) [22] and is based on theory for correlated U-statistics [24]. Let $\Phi^{-1}(.)$ denote the inverse cumulative distribution function of the standard normal distribution $\mathcal{N}(0, 1)$. Then, given a nominal significance level α, a one sided confidence interval for δ_j can be obtained as

$$\left[-1,\, \widehat{\delta}_j + \Phi^{-1}(1-\alpha)\widehat{\sigma}_{\delta_j}\right].$$

It can be shown that $\widehat{\delta}_j \sim N(\delta_j, \widehat{\sigma}_{\delta_j})$, and thus, taking the boundary of the null hypothesis in (1), $\delta_j = \epsilon$, the p-value for testing H_0 can be calculated as $p_j = P\left(Z < \widehat{\delta}_j\right)$ where $Z \sim N\left(\epsilon, \widehat{\sigma}_{\delta_j}\right)$. A p-value $p_j < \alpha$ therefore corresponds exactly to the case where the upper confidence interval of $\widehat{\delta}_j$ is less than ϵ.

Of course, the choice of ϵ is subject to debate. One could choose a fixed low value of ϵ *a priori* based on context or clinical guidance, but in the absence of prior knowledge, one can instead choose ϵ adaptively. Specifically, if the estimated treatment effect is $\widehat{U}_Y$, the significance level α and the desired power to detect a treatment effect based upon the candidate surrogate S_j is $(1-\beta)$, one may select ϵ as:

$$\epsilon = \max\left\{0, \widehat{u}_Y - u^*_{\alpha,\beta}\right\}, \tag{2}$$

where

$$u^*_{\alpha,\beta} = \frac{1}{2} - \sqrt{\frac{n_0+n_1+1}{12n_0n_1}}\left[\Phi^{-1}(\beta) - \Phi^{-1}(1-\alpha)\right].$$

The motivation behind this approach is that $u^*_{\alpha,\beta}$ (obtained with some algebra) is the value of U_{S_j} where we would have exactly $(1-\beta)$ power to detect a treatment effect on S_j. Defining ϵ as shown in (2) implies that we are willing to consider S_j as a surrogate for Y even if it is not as "good" as Y in terms of capturing the treatment effect, as long as it has a certain minimum power which we specify. That is, our threshold is $\widehat{u}_Y - u^*_{\alpha,\beta}$ and is determined by our desired power.

Overview of RISE

Our proposed approach comprises two steps. In the first, we apply the aforementioned rank-based procedure to each candidate surrogate S_j to screen $\boldsymbol{S}$ for the most promising candidates. In the second step, we evaluate the strength of the identified set of surrogates. To avoid overfitting, we use sample splitting to separate our full data into screening and evaluation sets, such that each step uses distinct data [25].

Step 1 - Rank-Based Screening

Given a significance level α and desired power $(1-\beta)$, we apply the previously detailed rank-based procedure to each surrogate S_j in the screening dataset, resulting in a point estimate $\widehat{\delta_j}$, its standard deviation $\widehat{\sigma}_{\delta_j}$, associated confidence interval and p-value. To control the excessive false discovery rate (FDR) among our identified candidate surrogates resulting from the high number of statistical tests, we perform a multiple testing correction on the p-values [26]. The subset of candidate surrogates, which we call $\mathcal{S}$, can then be selected as those whose adjusted p-values fall below α.

Step 2 - Evaluating Strength of Surrogate

In the second step, we propose to evaluate the strength of the set $\mathcal{S}$ by first reducing the dimension of $\mathcal{S}$ to a single marker through a weighted sum

$$\widehat{\gamma}_{\mathcal{S}} = \sum_{j\in\mathcal{S}} \left|\widehat{\delta_j}\right|^{-1} \bar{S}_j$$

where $\bar{S}_j$ is S_j standardised to have mean 0 and standard deviation 1, and the weights are the inverse of the estimated δ_j, such that stronger surrogates contribute more to the combined marker. We take the absolute value of the weights to avoid negative contributions where the treatment effect on the surrogate is slightly stronger than that on the primary outcome. Then, the rank-based procedure for a single surrogate is applied with $\widehat{\gamma}_{\mathcal{S}}$ in the evaluation dataset. If the p-value falls below α, we conclude that $\widehat{\gamma}_{\mathcal{S}}$ is a useful surrogate for Y.

2.3 Simulation Study Setup

We conducted a simulation study to evaluate the performance of our proposed two-step procedure under varying conditions and data-generating processes. The datasets were generated with $P = 500$ variables, a nominal significance level of $\alpha = 0.05$, and results summarised over $N_{\text{sim}} = 500$ simulations. Two primary scenarios were considered, each designed to assess different aspects of performance. In Scenario 1, no valid surrogates were generated. This setup allowed us to evaluate the false positive rate (FPR) – the proportion of false positives among all negatives. In Scenario 2, 10% of the surrogates were valid, enabling the empirical assessment of the false discovery proportion (FDP) – the proportion of false positives among all claimed positives – and the statistical power, defined as the proportion of positives found significant.

Definition of Valid Surrogates
By construction, the non-inferiority margin determines whether a variable is classified as a valid or invalid surrogate under our framework. Specifically, any S_j where $U_{S_j} < U_Y - \epsilon$ is deemed invalid; otherwise, it is considered valid. The true values of U_Y and U_{S_j}, denoted U_Y^* and $U_{S_j}^*$, can be derived analytically or through the asymptotic properties of U-statistics.

For our proposed procedure, invalid surrogates were generated as perfectly useless surrogates with $\widehat{U}_{S_j} = 0.5$, and ϵ was fixed at $\widehat{U}_Y - 0.5$. This setup allowed us to examine the p-value distribution at the boundary of the non-inferiority test and investigate how increasing the strength of surrogates beyond this boundary affects the test statistical power. It should be noted that, in practice, this choice of ϵ is unlikely to be useful for identifying surrogates that explain a substantial portion of the treatment effect on Y.

Data-Generating Processes
Let p_{invalid} and p_{valid} denote the numbers of invalid and valid surrogates, respectively. In Scenario 1, all 500 variables were invalid surrogates ($p_{\text{invalid}} = 500$ and $p_{\text{valid}} = 0$). In Scenario 2, 10% of the variables were valid surrogates ($p_{\text{invalid}} = 450$ and $p_{\text{valid}} = 50$). We considered two different data-generating processes (DGPs).

DGP 1: Multivariate Normal – All variables were generated from multivariate normal distributions. The responses followed $Y_a \sim \mathcal{N}(\mu_{y_a}, \sigma_{y_a})$, with $\mu_{y_1} = 3$, $\mu_{y_0} = 0$, and $\sigma_{y_a} = 1$. This setup resulted in a theoretical $U_Y^* = 0.985$, representing a strong treatment effect on Y. Invalid surrogates were generated as $S_{j,a} \sim \mathcal{N}_{p_{\text{invalid}}}(\boldsymbol{M}, \Sigma_{\text{invalid}})$, where $\boldsymbol{M} = (m_1, ..., m_{p_{\text{invalid}}})^T$, $m_j \sim U(0.5, 2.5)$, and $\Sigma_{\text{invalid}} = \text{diag}(\sigma_1, ..., \sigma_{p_{\text{invalid}}})$, with $\sigma_j \sim U(0.5, 2)$. Valid surrogates were generated by perturbing the true responses: $S_{j,a} = y_a + \mathcal{N}_{p\text{valid}}(\mathbf{0}, \Sigma_{\text{valid}})$, where $\Sigma_{\text{valid}} = \text{diag}(\sigma_{\text{valid}})$. The strength of surrogates was controlled by σ_{valid}, with larger values indicating weaker surrogates. Where the impact of multicollinearity was of interest, a constant σ_{corr} was added to the off-diagonal elements of Σ_{invalid} and $\sigma_{\text{corr}} * \sigma_{\text{valid}}$ to the off-diagonal elements of Σ_{valid}.

DGP 2: Complex Surrogate-Response Relationships – To introduce more complex invalid surrogate generation and surrogate-response relationships, responses were generated as in DGP 1, while invalid surrogates were sampled from exponential distributions: $S_{j,a} \sim \text{Exp}(\lambda_j)$, with $\lambda_j \sim U(0.5, 2.5)$. Valid surrogates were derived by perturbing a transformed response: $S_{j,a} = f(y_a) + \mathcal{N}_{p_{\text{valid}}}(\mathbf{0}, \Sigma_{\text{valid}})$, where $f(x) = x^3$, and Σ_{valid} was as defined earlier in DGP 1.

Evaluation Stage
In the second stage of our testing procedure, some subset of markers $S_j \in \mathcal{S}$ are combined to form a single marker $\widehat{\gamma}_{\mathcal{S}}$. This combination may consist of both true positives and false positives, in proportions ρ_{valid} and ρ_{invalid}, respectively. Although type I error and statistical power can be clearly defined in the case where we have either none or all false positives ($\rho_{\text{valid}} \in \{0, 1\}$), it is less straightforward when the components of $\widehat{\gamma}_{\mathcal{S}}$ are mixed ($\rho_{\text{valid}} \in (0, 1)$). Therefore, we opt to set $|\mathcal{S}| = 20$ and simply examine the distributions of p-values under varying ρ_{invalid}. Throughout, valid surrogates were generated with average strength $\widehat{U}_{S_j} = 0.9$.

3 Results

3.1 Simulation Results

Step 1 - Screening
We first examined the properties of the test under data generation process 1. In Scenario 1, where no valid surrogates were present, we examined the false positive rate (FPR) across various sample sizes in the uncorrelated setting. The empirical FPR remained close to the nominal level of 0.05 for sample sizes greater than 30, indicating a lower practical limit for the sample size and demonstrating that the procedure performs well even with small sample sizes (Figure 1). We then assessed the impact of correlation on the FPR for a fixed sample size of $n = 50$. In the absence of correlation, the FPR remained close to the nominal value with minimal variance across simulations. However, as correlation increased, the mean FPR decreased below the nominal value of 5% but its variance grew, with the highest correlation levels leading to a handful of extreme outliers (Figure 2). In Scenario 2, where there was 10% of valid surrogates, we evaluated the empirical FDP and empirical power (or true positive rate) across varying surrogate strength values ($\widehat{U}_S = 0.55, 0.60, ..., 0.95, U_Y$) and sample sizes ($n = 30, 50, 100$) in the

uncorrelated setting. As expected, empirical power increased to nearly 1, while empirical FDR decreased to its minimum value as the average surrogate strength increased (Figure 3). When examining the impact of correlation in Scenario 2 for a fixed sample size of $n = 50$ and average surrogate strength of $\widehat{U}_S = 0.9$, we found that the FDP decreased on average, but became more variable at higher correlation levels. However, empirical power appeared to be largely unaffected by correlation (Supporting Information Figure S1). We also assessed the effect of three multiple testing correction methods: Benjamini-Hochberg (B-H), Bonferroni, and Benjamini-Yekutieli (B-Y) [27, 28, 29]. As expected, all three of the procedures controlled the FDR well and resulted in satisfactory power at high surrogate strengths (Supporting Information Figure S2). The Bonferroni and B-Y procedures were found to offer stricter control of the FDR compared to the B-H procedure, which provided more balance between controlling the expected FDR and maintaining the power to detect true signals.

We next examined the properties of the test under the more complex data generation process 2. Overall, the properties of the test remained similar to those observed under DGP 1, with the only notable difference being in the observed FPR, which was more stable across different levels of inter-predictor correlation (Supporting Information Figures S3, S4, S5).

Step 2 - Evaluation
In the evaluation stage, we examined the distribution of p-values as a function of the FDP in $\widehat{\gamma}_{\mathcal{S}}$. For both data generation processes, When the FDP was low (≤ 0.2), the null hypothesis was always rejected (indicating that $\widehat{\gamma}_{\mathcal{S}}$ was a strong surrogate). In contrast, the null hypothesis was never rejected when the FDP was too high (≥ 0.6). When $\widehat{\gamma}_{\mathcal{S}}$ contained a balanced mixture of false and true positives ($0.3 < \rho_{\text{invalid}} \leq 0.5$), the null hypothesis was mostly not rejected, but p-values exhibited higher variance (Figure 4, Supporting Information Figure S6). This is desirable behaviour, as we have shown the false discovery proportion to be low in our setup subject to the 3 multiple testing corrections tested (Supporting Information Figure S2), which will lead to rejection of the null hypothesis for $\widehat{\gamma}_{\mathcal{S}}$. In addition, in the event of an elevated false discovery proportion, the null hypothesis is unlikely to be rejected.

3.2 Application to Influenza Vaccination Data

We applied RISE to publicly available gene expression and immune response data to identify and evaluate potential surrogate markers of the immune response to the trivalent inactivated influenza vaccine (TIV). These data are available from the ImmPort platform [30] (immport.org) under study accession number SDY1276 (entited *time series of global gene expression after trivalent influenza vaccination in humans*). TIV is a seasonal flu vaccine containing inactivated forms of three influenza virus strains, designed to stimulate immune protection without causing infection [31]. We applied RISE to a study examining the response of young, healthy adult volunteers to the 2008-2009 TIV formulation, which is designed to protect against two strains of influenza A and one strain of influenza B. Due to the previously reported variability in response to influenza vaccination at both the immune and transcriptomic levels based on sex [32, 33], we further subsetted the data to include only female subjects.

In the absence of a true placebo group, we considered the control group to be the baseline measurements of the primary response and surrogate marker candidates taken just prior to vaccination. For this illustration, the primary outcome was defined as the mean strain-specific neutralising antibody titres, measured at baseline for the control samples and at day 28 post-vaccination for the treated samples. Gene expression in whole blood cells was assessed using microarray technology. Candidate surrogate markers were defined as gene expression measurements, taken at baseline for the control samples and at day 1 post-vaccination for the treated samples.

The dataset comprised observations on 106 unique individuals, where three lacked a gene expression measurement at day 1 post-vaccination. Therefore, the final data consisted of 209 observations, including 106 control samples and 103 treated samples. The samples were randomly assigned into screening and evaluation datasets at a ratio of 85:15 respectively. The significance level was held at $\alpha = 0.05$, and the desired power in the screening stage was fixed at 0.90. The Bonferroni procedure was used to correct the resulting p-values. The estimated value of U_Y was 0.95, reflecting a strong neutralising antibody response to TIV, and corresponding to a non-inferiority threshold of $\epsilon = 0.31$. Among the $10,086$ genes in the expression data, 235 had an adjusted p-value below 0.05. For illustration and brevity, we display the top 20 of these 235 genes sorted by adjusted p-value in Table 1, along with the estimates for $U_Y - U_{S_j} = \delta_j$, corresponding confidence intervals, standard deviations σ_{δ_j}, and both raw and adjusted p-values. The full list of genes can be found in Supporting Information Table S1.

In the evaluation phase, the identified set of 235 genes from Step 1 of RISE were combined using a standardised weighted sum to form a single predictor, denoted γ_S. In the evaluation dataset, the estimated value of U_Y was 0.99, corresponding to $\epsilon = 0.15$ for a desired 0.90 powered test based on γ_S. The value of δ was found to be -0.0063 (95% C.I. $[-1, 0.015]$), with a standard deviation of 0.013, yielding a p-value of $2e-32$. The negative value of δ reflects the fact that the point estimate of the treatment effect on the gene expression is slightly stronger than that on the antibody response. These results suggest that the constructed γ_S is a reasonable surrogate for the neutralising antibody response to the 2008-2009 TIV amongst females. This is further illustrated in Figure 5, which plots the ranks of the true response against γ_S, showing strong positive correlation between the antibody ranks and the new surrogate ranks (Spearman rank correlation coefficient $\rho = 0.79$).

In our application, the non-inferiority threshold for screening was substantial, even at a desired power of 0.90, resulting in a high number of significant genes. This outcome is unsurprising given the large effect size of the primary outcome and the larger sample size. To control for multiple testing, we applied the Bonferroni correction, the strictest method considered, which consequently yielded a more parsimonious gene signature. We additionally conducted a sensitivity analysis to evaluate the robustness of the results to the value of ϵ (Supporting Information Table S2). Indeed, choosing a stricter non-inferiority margin results in more parsimonious signatures which are equally strong surrogates as those constructed with more predictors. For example, the top four genes alone produce an equally strong γ_S surrogate as that with 235 genes. These results likely reflect the high degree of shared information between genes in the same biological pathways. Indeed, the biological functions of the 235 genes were examined using DAVID bioinformatics to identify ontological terms which were significantly over-represented in the list. This revealed a significant proportion of these genes to be related to innate antiviral processes, providing a clear immunological interpretation of the signature (Table 2); we discuss this further in the Discussion.

In conclusion, we identified a subset of genes whose early post-vaccination expression may serve as a promising surrogate for the mid-term immunogenicity of an inactivated influenza vaccine in healthy adult females. This provides a basis for further validation and illustrates RISE's practicality as a framework for exploring surrogate markers in clinical studies with high-dimensional candidate markers.

4 Discussion

Surrogate markers can provide significant advantages in the conduct of randomised clinical trials, particularly those evaluating vaccine immunogenicity. High-dimensional molecular markers are promising candidates for surrogates in this context due to their biological relevance and practical utility. However, existing methods for identifying and validating surrogate markers typically break down in high-dimensional contexts, necessitate large sample sizes, or rely on restrictive parametric assumptions. In this study, we introduced RISE – a novel two-step method for identifying and evaluating high-dimensional surrogate markers, applied in the context of a vaccine clinical trial.

Our approach builds upon existing rank-based methodologies by adapting them for high-dimensional settings through a combination of univariate testing and dimension reduction, followed by evaluation using independent data. RISE effectively addresses several key challenges associated with evaluating high-dimensional molecular surrogates, such as the large number of candidate surrogates, limited sample sizes, and the need for false discovery rate control. The initial screening step utilises a non-parametric, rank-based univariate test to evaluate whether each variable performs at least as well as the primary outcome in demonstrating a treatment effect up to some small margin. As discussed in the study introducing the rank-based approach for single surrogate markers [22], this method offers several advantages that are particularly relevant in high-dimensional vaccine trials. First, the test enables robust and valid inference even in small sample scenarios, where assumptions like linearity and normality are difficult to verify. Second, being rank-based, the test is invariant to data transformations and robust to outliers, which is crucial in high-dimensional data often subjected to various transformations prior to analysis. Finally, by comparing entire rank distributions rather than relying on summary statistics like the mean, this method provides a more comprehensive assessment of surrogate strength. The evaluation step in RISE then uses a weighted combination of the screened predictors to form a synthetic biomarker.

Our simulation studies illustrate the favourable properties of RISE's screening process. We demonstrated that the test procedure is valid and well-calibrated, although caution is required for very small samples or when inter-predictor correlations are high, as the false positive rate may slightly deviate from the nominal level. Additionally, we explored how surrogate strength and sample size influence empirical power and false positive rates. The test exhibited high power to detect true positives and minimised false positives when surrogates were strong, even with small sample sizes. This is encouraging, as in practice,

we are primarily concerned with identifying the strongest surrogates. These findings also emphasise the importance of multiple testing corrections in order to control the elevated false positive rate in situations with a low proportion of true positives amongst high-dimensional predictors.

In applying RISE to a vaccine trial, our objective was to identify early gene expression markers that could serve as surrogates for the neutralising antibody response following immunisation with a seasonal trivalent inactivated influenza vaccine (TIV). A signature of 235 genes was identified, with day 1 post-injection expression appearing to function individually as effective surrogates in the screening data subset. A standardised, weighted combination of these 235 genes was then evaluated on independent data as a viable candidate to replace the day 28 neutralising antibody response. The biological functions of these genes were explored using DAVID [34], a bioinformatics tool that summarises biological functions associated with a gene group by identifying over-represented terms compared to those expected by random sampling of the same number of genes. This analysis revealed that many genes in the signature were linked to antiviral defence and innate immunity pathways (Table 2). In particular, numerous genes in the list are known to regulate or be stimulated by interferons, a family of proteins that interfere with viral infections, making these genes sensitive indicators of innate immune activation. Genes in this signature related to the interferon response include interferon-induced genes (IFI6, IFI16, IFI35, IFI44, IFI44L, IFIT1, IFIT2, IFIT3, IFIT5), the STAT family (STAT1, STAT2), interferon regulatory factors (IRF1, IRF2, IRF7, IRF9), the OAS family (OAS1, OAS2, OAS3, OASL), MX proteins (MX1, MX2), viral sensors (DDX58, IFIH1), and other interferon-stimulated genes (ISG20, GBP1, GBP2, BST2, RSAD2, XAF1, TRIM21, TRIM22, TRIM5). Further work is required to determine whether activation of these pathways can robustly predict the neutralising antibody response at both the trial and individual levels, across individuals with varying instrinsic characteristics and different formulations of TIV.

While this study represents a significant advancement in non-parametric methods for identifying high-dimensional surrogate markers, several limitations must be acknowledged. The first is the dependence on the inferiority margin ϵ for selecting surrogate markers during screening. While we propose a data-driven approach linking ϵ to the significance level and desired power, ϵ itself remains ad hoc and challenging to interpret compared to commonly used measures in surrogate analysis such at the proportion of treatment effect explained or relative effect. Although the value of ϵ should not be chosen post-hoc based on the resulting evaluation metrics, we recommend conducting sensitivity analyses to evaluate how different ϵ values influence overall conclusions. Additionally, the method of combining candidate markers into a single surrogate warrants further consideration. We propose a weighted, standardised sum of the markers that pass the screening stage, with weights proportional to their strength as surrogates. While this approach is intuitive, one may argue that the resulting surrogate is artificial and/or has limited biological interpretation.

Although the rank-based approach offers many advantages, a notable disadvantage is that it requires a continuous outcome. In many contexts, the primary outcome may be binary (for example, protected against disease or not), in which case, RISE cannot be used to assess possible surrogates. Indeed, the choice of outcome in our data application was the neutralising antibody levels, a continuous marker whose quantity and duration has been used itself as a surrogate marker to study the efficacy of TIV. This results in the identification of markers which are, in reality, surrogates of a surrogate. While this approach is pragmatic in the absence of clinical endpoints, it introduces limitations, including a potentially weaker or indirect relationship with the ultimate outcome of interest, and the risk of identifying markers that lack generalisability or biological relevance to true disease protection. It is also crucial to emphasise that the markers identified by RISE are statistical surrogates rather than mechanistic ones, meaning they are associated with both the vaccine and its induced neutralising antibody response, but may not necessarily directly reflect the underlying biological mechanisms [35]. This distinction is vital in the context of gene expression studies, where complex co-expression patterns and regulation cycles may lead to variables associated with an intervention and its outcome, but which are not directly involved in the mechanism.

Finally, RISE's univariate screening does not account for gene-gene interactions, which are critical for fully understanding the relationship between vaccine-induced gene expression patterns and the resulting immune response. It is well established that genes do not function in isolation but as components of biological pathways [36]. Focusing on these pathways instead of individual genes may yield greater biological insight and robustness against individual and experimental variability. In addition, gene expression responses may demonstrate temporal heterogeneity between individuals. Therefore, directions for future development to improve the robustness of the RISE methodology include extension to account for pathway-level trends as well as the consideration of more complex experimental designs, such as repeated or longitudinal measurements of the high-dimensional surrogate candidates.

5 Acknowledgements

This work is part of AH's PhD thesis at the University of Bordeaux, co-supervised by BPH and RT. AH is supported by the University of Bordeaux's Digital Public Health Graduate School, funded by France's PIA 3 scheme (Investments for the Future – Project reference: 17-EURE-0019), the Programme et Equipement Prioritaire de Recherche Santé Numérique (PEPR SN) project SMATCH (ref: 22-PESN-0003), and INRIA's DESTRIER associate team, within the program Inria@SiliconValley (ref: DRI-01221). The authors thank the Human Immunology Project Consortium for providing the ImmPort platform for open-access immunology data. We also acknowledge the investigators who contributed data for study SDY1276, supported by the NIAID Program Research Project Grant (Parent R01) and the Viral Respiratory Pathogens Research Unit (VRPRU)-266030039. The authors benefited from the Rank-Based Identification of Surrogates in Small Ebola Studies (RISE) Symposium, organized by LP and BPH at the University of Texas at Austin, USA. This event was supported by the Dr. Cecile DeWitt-Morette France-UT Endowed Excellence Fund, which promotes scholarly collaborations between UT Austin and institutions in France. The authors disclose that generative AI tools were used to refine the phrasing of certain sections of the manuscript.

References

[1] Robin Christensen, Oriana Ciani, Anthony M. Manyara, and Rod S. Taylor. Surrogate endpoints: a key concept in clinical epidemiology. *Journal of Clinical Epidemiology*, 167:111242, March 2024.

[2] Peter B. Gilbert, Youyi Fong, Nima S. Hejazi, Avi Kenny, Ying Huang, Marco Carone, David Benkeser, and Dean Follmann. Four statistical frameworks for assessing an immune correlate of protection (surrogate endpoint) from a randomized, controlled, vaccine efficacy trial. *Vaccine*, 42(9):2181–2190, April 2024.

[3] Stanley A. Plotkin. Correlates of protection induced by vaccination. *Clinical and Vaccine Immunology*, 17(7):1055–1065, July 2010.

[4] January Weiner, Stefan H.E. Kaufmann, and Jeroen Maertzdorf. High-throughput data analysis and data integration for vaccine trials. *Vaccine*, 33(40):5249–5255, September 2015.

[5] Jue Hou, Shuhui Wang, Manxue Jia, Dan Li, Ying Liu, Zhengpeng Li, Hong Zhu, Huifang Xu, Meiping Sun, Li Lu, Zhinan Zhou, Hong Peng, Qichen Zhang, Shihong Fu, Guodong Liang, Lena Yao, Xuesong Yu, Lindsay N. Carpp, Yunda Huang, Julie McElrath, Steve Self, and Yiming Shao. A systems vaccinology approach reveals temporal transcriptomic changes of immune responses to the yellow fever 17d vaccine. *The Journal of Immunology*, 199(4):1476–1489, August 2017.

[6] David Furman and Mark M. Davis. New approaches to understanding the immune response to vaccination and infection. *Vaccine*, 33(40):5271–5281, September 2015.

[7] Mengya Liu, Qing Li, Jianchang Lin, Yunzhi Lin, and Elaine Hoffman. Innovative trial designs and analyses for vaccine clinical development. *Contemporary Clinical Trials*, 100:106225, January 2021.

[8] Troy D Querec, Rama S Akondy, Eva K Lee, Weiping Cao, Helder I Nakaya, Dirk Teuwen, Ali Pirani, Kim Gernert, Jiusheng Deng, Bruz Marzolf, Kathleen Kennedy, Haiyan Wu, Soumaya Bennouna, Herold Oluoch, Joseph Miller, Ricardo Z Vencio, Mark Mulligan, Alan Aderem, Rafi Ahmed, and Bali Pulendran. Systems biology approach predicts immunogenicity of the yellow fever vaccine in humans. *Nature Immunology*, 10(1):116–125, November 2008.

[9] Dmitri Kazmin, Helder I. Nakaya, Eva K. Lee, Matthew J. Johnson, Robbert van der Most, Robert A. van den Berg, W. Ripley Ballou, Erik Jongert, Ulrike Wille-Reece, Christian Ockenhouse, Alan Aderem, Daniel E. Zak, Jerald Sadoff, Jenny Hendriks, Jens Wrammert, Rafi Ahmed, and Bali Pulendran. Systems analysis of protective immune responses to rts,s malaria vaccination in humans. *Proceedings of the National Academy of Sciences*, 114(9):2425–2430, February 2017.

[10] Helder I Nakaya, Jens Wrammert, Eva K Lee, Luigi Racioppi, Stephanie Marie-Kunze, W Nicholas Haining, Anthony R Means, Sudhir P Kasturi, Nooruddin Khan, Gui-Mei Li, Megan McCausland, Vibhu Kanchan, Kenneth E Kokko, Shuzhao Li, Rivka Elbein, Aneesh K Mehta, Alan Aderem, Kanta Subbarao, Rafi Ahmed, and Bali Pulendran. Systems biology of vaccination for seasonal influenza in humans. *Nature Immunology*, 12(8):786–795, July 2011.

[11] Ross L. Prentice. Surrogate endpoints in clinical trials: Definition and operational criteria. *Statistics in Medicine*, 8(4):431–440, April 1989.

[12] Laurence S. Freedman, Barry I. Graubard, and Arthur Schatzkin. Statistical validation of intermediate endpoints for chronic diseases. *Statistics in Medicine*, 11(2):167–178, January 1992.

[13] D. Y. LIN, T. R. FLEMING, and V. DE GRUTTOLA. Estimating the proportion of treatment effect explained by a surrogate marker. *Statistics in Medicine*, 16(13):1515–1527, July 1997.

[14] Yue Wang and Jeremy M. G. Taylor. A measure of the proportion of treatment effect explained by a surrogate marker. *Biometrics*, 58(4):803–812, December 2002.

[15] Zhengqing Li, Michael P. Meredith, and Mohammad S. Hoseyni. A method to assess the proportion of treatment effect explained by a surrogate endpoint. *Statistics in Medicine*, 20(21):3175–3188, October 2001.

[16] Layla Parast, Mary M. McDermott, and Lu Tian. Robust estimation of the proportion of treatment effect explained by surrogate marker information. *Statistics in Medicine*, 35(10):1637–1653, December 2015.

[17] Emily K. Roberts, Michael R. Elliott, and Jeremy M. G. Taylor. Surrogacy validation for time-to-event outcomes with illness-death frailty models. *Biometrical Journal*, 66(1), September 2023.

[18] M. Buyse, G. Molenberghs, T. Burzykowski, D. Renard, and H. Geys. The validation of surrogate endpoints in meta-analyses of randomized experiments. *Biostatistics*, 1(1):49–67, March 2000.

[19] Geert Molenberghs, Marc Buyse, Helena Geys, Didier Renard, Tomasz Burzykowski, and Ariel Alonso. Statistical challenges in the evaluation of surrogate endpoints in randomized trials. *Controlled Clinical Trials*, 23(6):607–625, December 2002.

[20] Denis Agniel and Layla Parast. Evaluation of longitudinal surrogate markers. *Biometrics*, 77(2):477–489, June 2020.

[21] Ruixuan Rachel Zhou, Sihai Dave Zhao, and Layla Parast. Estimation of the proportion of treatment effect explained by a high-dimensional surrogate. *Statistics in Medicine*, 41(12):2227–2246, February 2022.

[22] Layla Parast, Tianxi Cai, and Lu Tian. A rank-based approach to evaluate a surrogate marker in a small sample setting. *Biometrics*, 80(1), January 2024.

[23] H. B. Mann and D. R. Whitney. On a test of whether one of two random variables is stochastically larger than the other. *The Annals of Mathematical Statistics*, 18(1):50–60, March 1947.

[24] Elizabeth R. DeLong, David M. DeLong, and Daniel L. Clarke-Pearson. Comparing the areas under two or more correlated receiver operating characteristic curves: A nonparametric approach. *Biometrics*, 44(3):837, September 1988.

[25] Tali M. Ball, Lindsay M. Squeglia, Susan F. Tapert, and Martin P. Paulus. Double dipping in machine learning: Problems and solutions. *Biological Psychiatry: Cognitive Neuroscience and Neuroimaging*, 5(3):261–263, March 2020.

[26] Ralf Bender and Stefan Lange. Adjusting for multiple testing—when and how? *Journal of Clinical Epidemiology*, 54(4):343–349, April 2001.

[27] Yoav Benjamini and Yosef Hochberg. Controlling the false discovery rate: A practical and powerful approach to multiple testing. *Journal of the Royal Statistical Society Series B: Statistical Methodology*, 57(1):289–300, January 1995.

[28] Olive Jean Dunn. Multiple comparisons among means. *Journal of the American Statistical Association*, 56(293):52–64, March 1961.

[29] Yoav Benjamini and Daniel Yekutieli. The control of the false discovery rate in multiple testing under dependency. *The Annals of Statistics*, 29(4), August 2001.

[30] Sanchita Bhattacharya, Patrick Dunn, Cristel G. Thomas, Barry Smith, Henry Schaefer, Jieming Chen, Zicheng Hu, Kelly A. Zalocusky, Ravi D. Shankar, Shai S. Shen-Orr, Elizabeth Thomson, Jeffrey Wiser, and Atul J. Butte. Immport, toward repurposing of open access immunological assay data for translational and clinical research. *Scientific Data*, 5(1), February 2018.

[31] Sook-San Wong and Richard J. Webby. Traditional and new influenza vaccines. *Clinical Microbiology Reviews*, 26(3):476–492, July 2013.

[32] David Furman, Boris P. Hejblum, Noah Simon, Vladimir Jojic, Cornelia L. Dekker, Rodolphe Thiébaut, Robert J. Tibshirani, and Mark M. Davis. Systems analysis of sex differences reveals an immunosuppressive role for testosterone in the response to influenza vaccination. *Proceedings of the National Academy of Sciences*, 111(2):869–874, December 2013.

[33] Feng Wen, Jinyue Guo, Zhili Li, and Shujian Huang. Sex-specific patterns of gene expression following influenza vaccination. *Scientific Reports*, 8(1), September 2018.

[34] Da Wei Huang, Brad T Sherman, and Richard A Lempicki. Systematic and integrative analysis of large gene lists using david bioinformatics resources. *Nature Protocols*, 4(1):44–57, December 2008.

[35] S. A. Plotkin and P. B. Gilbert. Nomenclature for immune correlates of protection after vaccination. *Clinical Infectious Diseases*, 54(11):1615–1617, March 2012.

[36] Yered Pita-Juárez, Gabriel Altschuler, Sokratis Kariotis, Wenbin Wei, Katjuša Koler, Claire Green, Rudolph E. Tanzi, and Winston Hide. The pathway coexpression network: Revealing pathway relationships. *PLOS Computational Biology*, 14(3):e1006042, March 2018.

Table 1: Screening results from the data application - top 20 genes by adjusted p-values.

Gene	$\boldsymbol{\delta}$ **(95% C.I.)**	$\boldsymbol{\sigma_\delta}$	**Unadjusted p-value**	**Bonferroni Adjusted p-value**
PSME1	-0.037 (-1, -0.011)	0.016	6.3e-109	6.4e-105
NPC2	-0.035 (-1, -0.009)	0.016	1.2e-108	1.2e-104
VAMP5	-0.03 (-1, -0.004)	0.016	7.3e-102	7.4e-98
MYOF	-0.023 (-1, 0.005)	0.017	9.5e-91	9.6e-87
WARS1	-0.026 (-1, 0.002)	0.017	6.4e-88	6.4e-84
UBE2L6	-0.026 (-1, 0.005)	0.018	8.4e-76	8.4e-72
SERPING1	-0.022 (-1, 0.009)	0.019	1.8e-70	1.8e-66
SCO2	-0.017 (-1, 0.015)	0.019	9.7e-68	9.8e-64
STAT1	-0.019 (-1, 0.013)	0.019	1.0e-66	1.0e-62
IFI35	-0.018 (-1, 0.015)	0.020	1.4e-62	1.4e-58
STAT2	-0.016 (-1, 0.018)	0.020	6.3e-60	6.3e-56
GBP1	-0.011 (-1, 0.023)	0.020	2.6e-57	2.6e-53
RHBDF2	-0.008 (-1, 0.027)	0.021	1.6e-52	1.6e-48
GBP2	-0.004 (-1, 0.032)	0.022	2.0e-49	2.0e-45
TYMP	-0.004 (-1, 0.032)	0.022	7.3e-48	7.4e-44
IRF7	-0.003 (-1, 0.033)	0.022	1.7e-47	1.7e-43
XAF1	0.003 (-1, 0.04)	0.022	4.2e-45	4.3e-41
ADAP2	0.009 (-1, 0.045)	0.022	3.7e-44	3.8e-40
ATF5	0.008 (-1, 0.045)	0.023	7.4e-42	7.4e-38
SP140	0.004 (-1, 0.042)	0.023	2.4e-41	2.5e-37

Table 2: Functional annotation of 235 significant genes using DAVID.

Term	**Number of genes**	**B-H Adjusted p-value**
KW-0051-Antiviral defense	37	3.1e-33
GO:0051607-defense response to virus	43	5.6e-31
KW-0391-Immunity	59	1.1e-27
KW-0399-Innate immunity	45	4.2e-22
GO:0045071-negative regulation of viral genome replication	20	2.1e-19
GO:0045087-innate immune response	43	5.7e-18
GO:0009615-response to virus	24	2.3e-15
hsa05164:Influenza A	23	1.0e-10
GO:0034341-response to type II interferon	11	1.9e-09
hsa04621:NOD-like receptor signaling pathway	22	8.9e-10

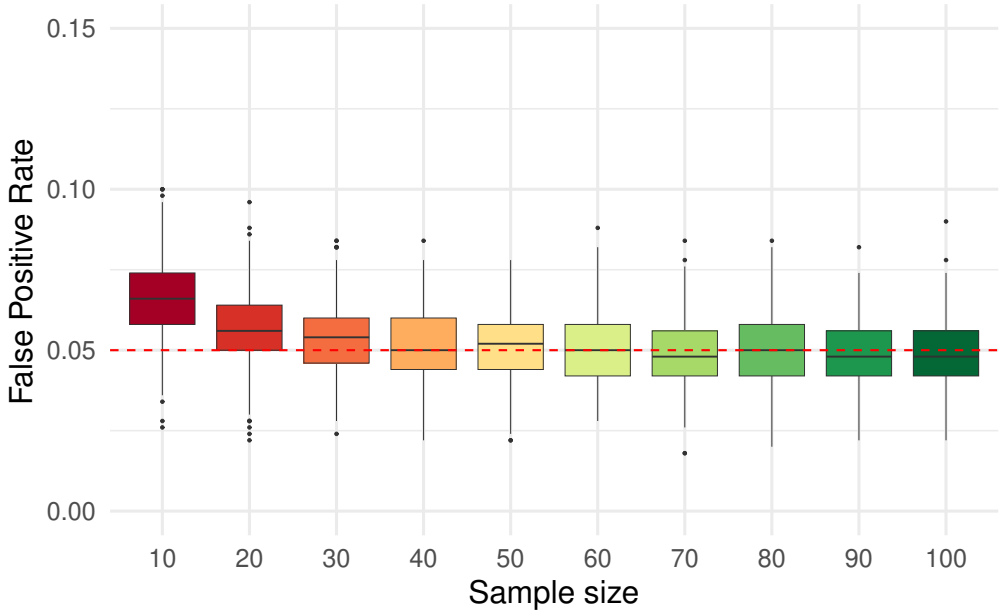

Figure 1: Data generation process 1, scenario 1: boxplots of observed false positive rates against different sample sizes in the uncorrelated setting. The nominal significance level $\alpha = 0.05$ is plotted as a dashed red line.

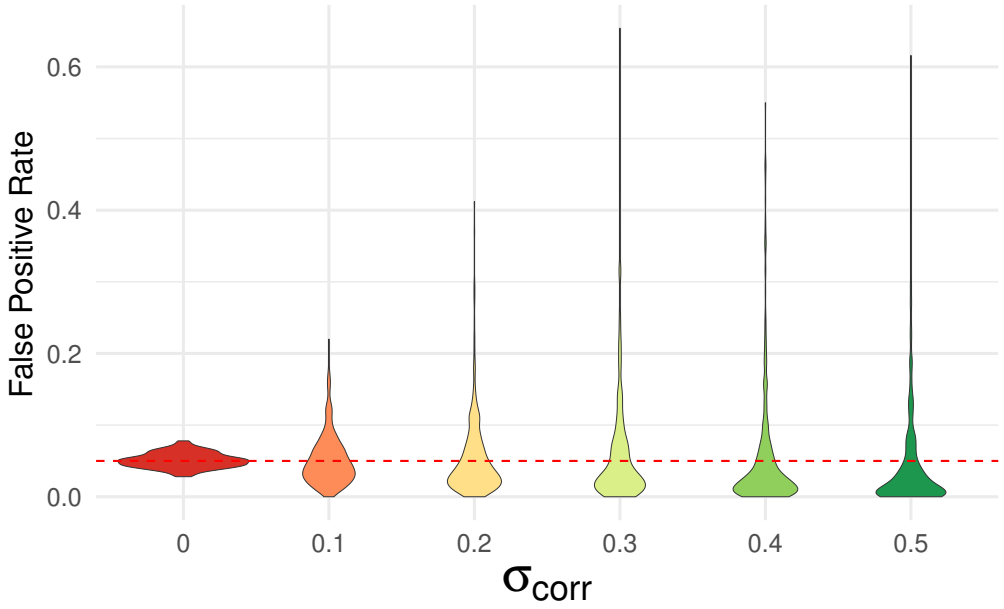

Figure 2: Data generation process 1, scenario 1: violin plots of observed false positive rates against different levels of correlation across 500 simulations for a fixed sample size of $n = 50$. Increasing the σ_{corr} parameter increases the inter-predictor correlation. The nominal significance level $\alpha = 0.05$ is plotted as a dashed red line.

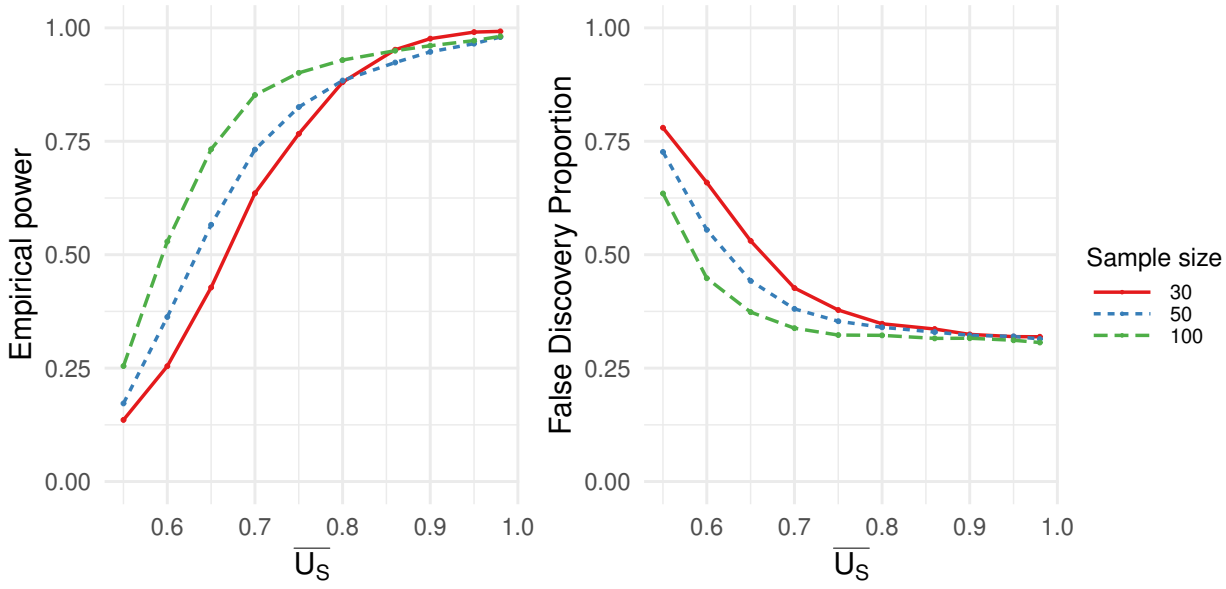

Figure 3: Data generation process 1, scenario 2: empirical power (left) and false discovery proportion (right) prior to multiple testing corrections as a function of average surrogate strength ($\bar{U_S}$) for three different sample sizes.

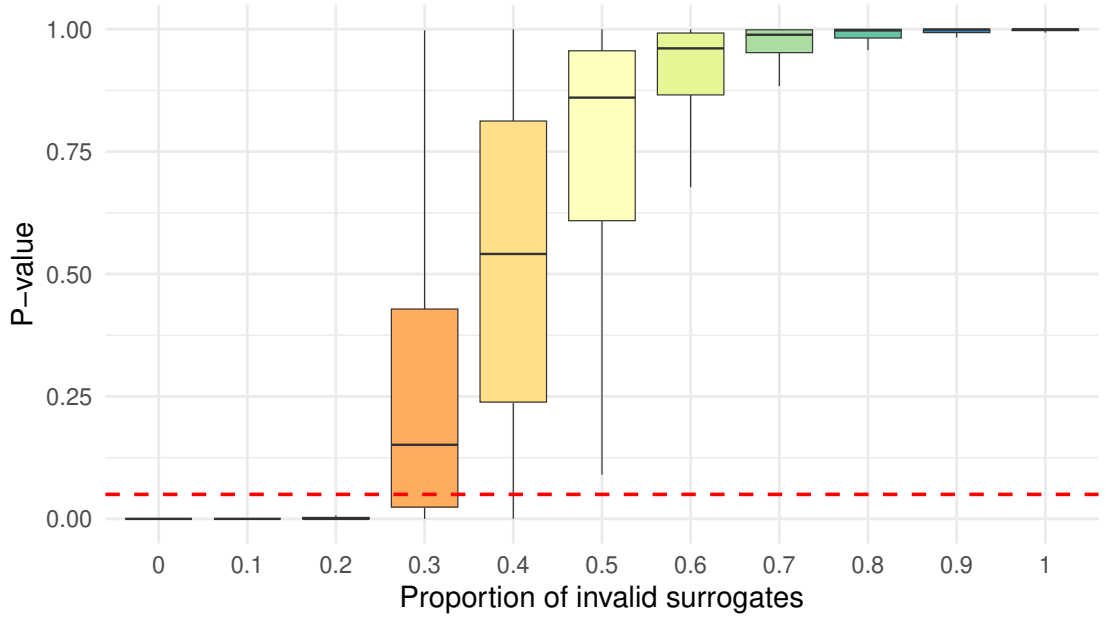

Figure 4: Data generation process 1: the distributions of the p-values in the evaluation step are examined as a function of the false discovery proportion which make up $\widehat{\gamma}_{\mathcal{S}}$, which consists of a combination of 20 predictors. The sample size is $n = 50$ and the valid surrogate strength is $\widehat{U_{S_j}} = 0.9$. The nominal significance level $\alpha = 0.05$ is plotted as a dashed red line. Desired power for the new surrogate was fixed at 80%.

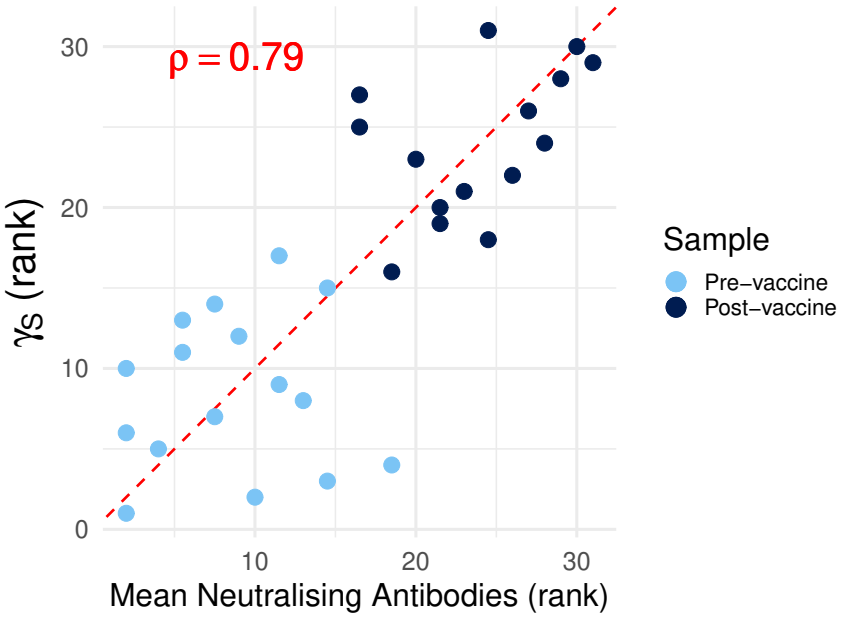

Figure 5: Ranks of the mean neutralising antibodies against the ranks of the constructed 235-gene-combination surrogate marker in the evaluation dataset. The Spearman rank correlation coefficient is 0.79, indicating strong positive correlation.

Supporting Information: Rank-Based Identification of High-dimensional Surrogate Markers: Application to Vaccinology

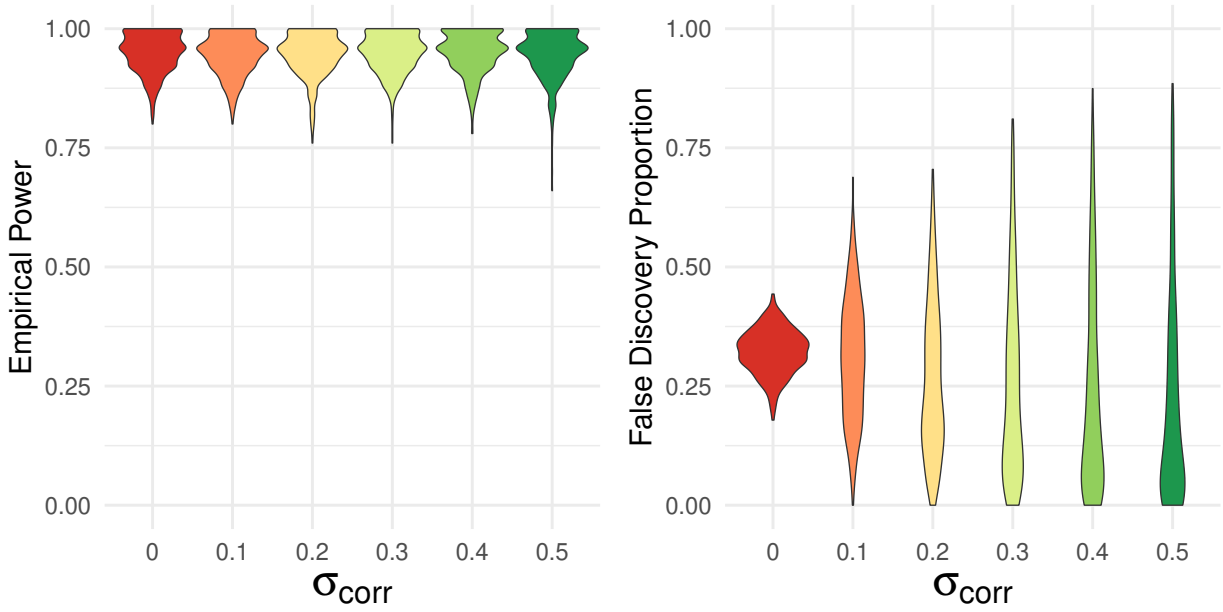

Figure S1: Data generation process 1, scenario 2: violin plots of empirical power (left) and false discovery proportion (right) prior to multiple testing corrections for a fixed sample size $n = 50$ and average surrogate strength $\bar{U}_S = 0.9$ for different values of inter-predictor correlation.

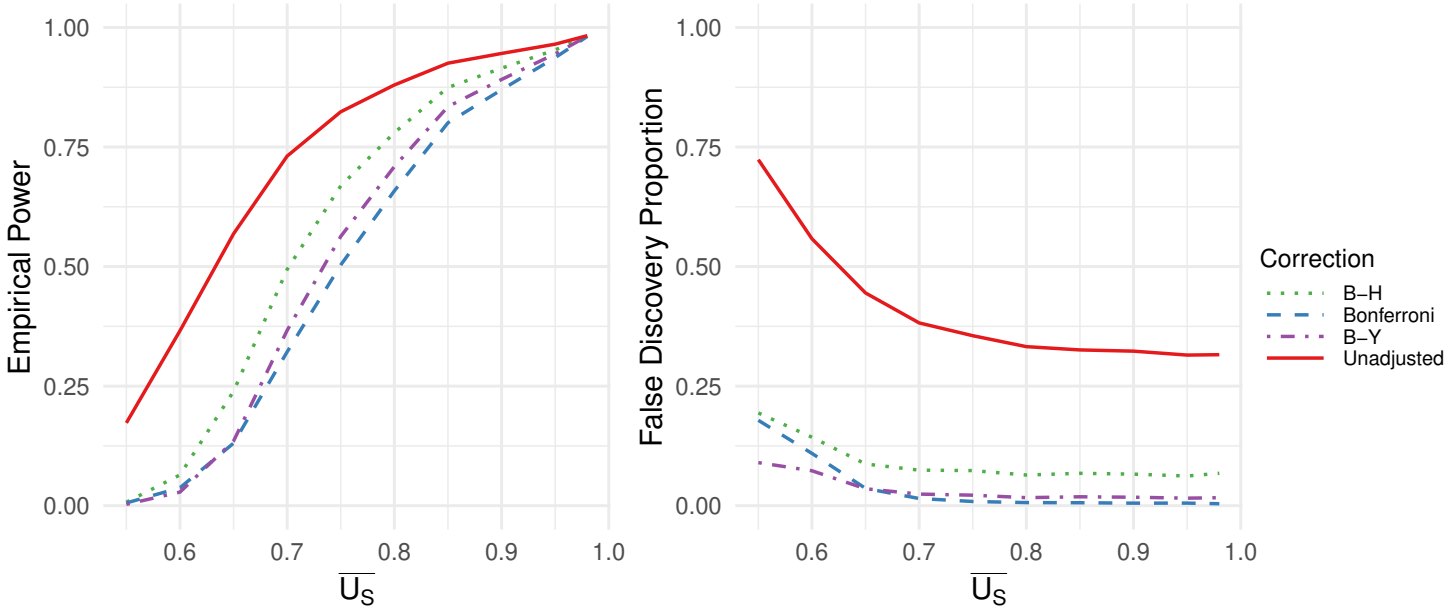

Figure S2: Data generation process 1, scenario 2: Empirical power (left) and false discovery proportion (right) prior to multiple testing corrections as a function of average surrogate strength for different multiple testing corrections (Benjamini-Hochberg, Bonferroni, Benjamini-Yekutieli, Unadjusted) for a fixed sample size $n = 50$.

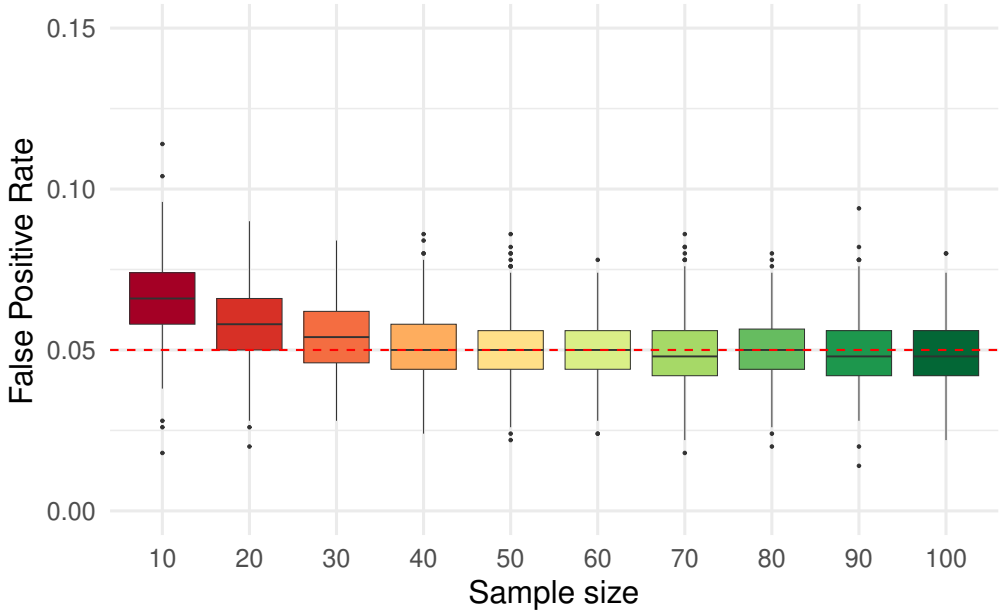

Figure S3: Data generation process 2, scenario 1: boxplots of observed false positive rates against different sample sizes in the uncorrelated setting. The nominal significance level $\alpha = 0.05$ is plotted as a dashed red line.

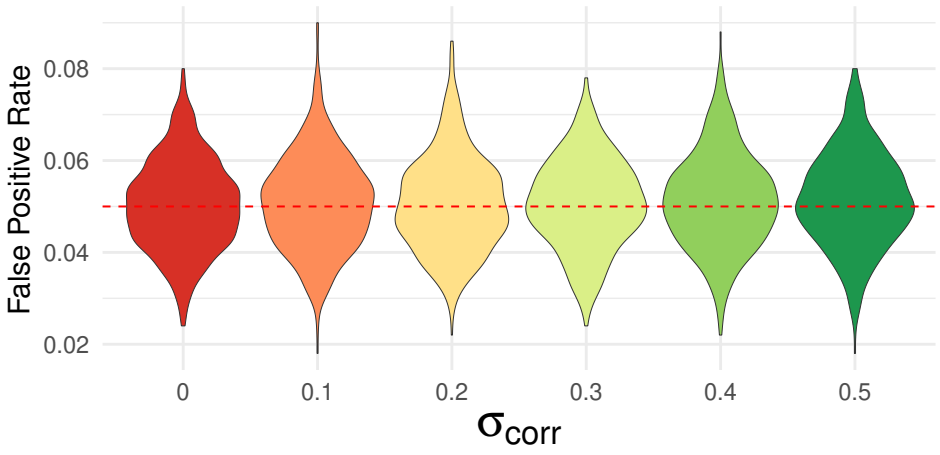

Figure S4: Data generation process 2, scenario 1: violin plots of observed false positive rates against different levels of correlation prior to multiple testing corrections across 500 simulations for a fixed sample size of $n = 50$. The nominal significance level $\alpha = 0.05$ is plotted as a dashed red line.

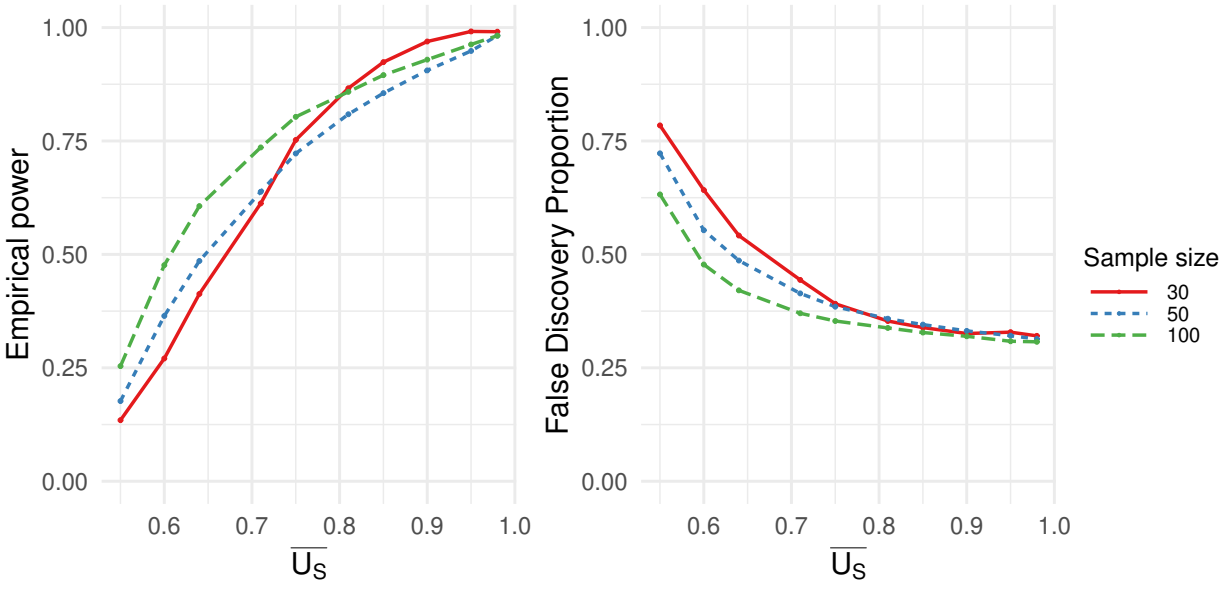

Figure S5: Data generation process 2, scenario 2: empirical power (left) and false discovery proportion (right) prior to multiple testing corrections as a function of average surrogate strength for three different sample sizes.

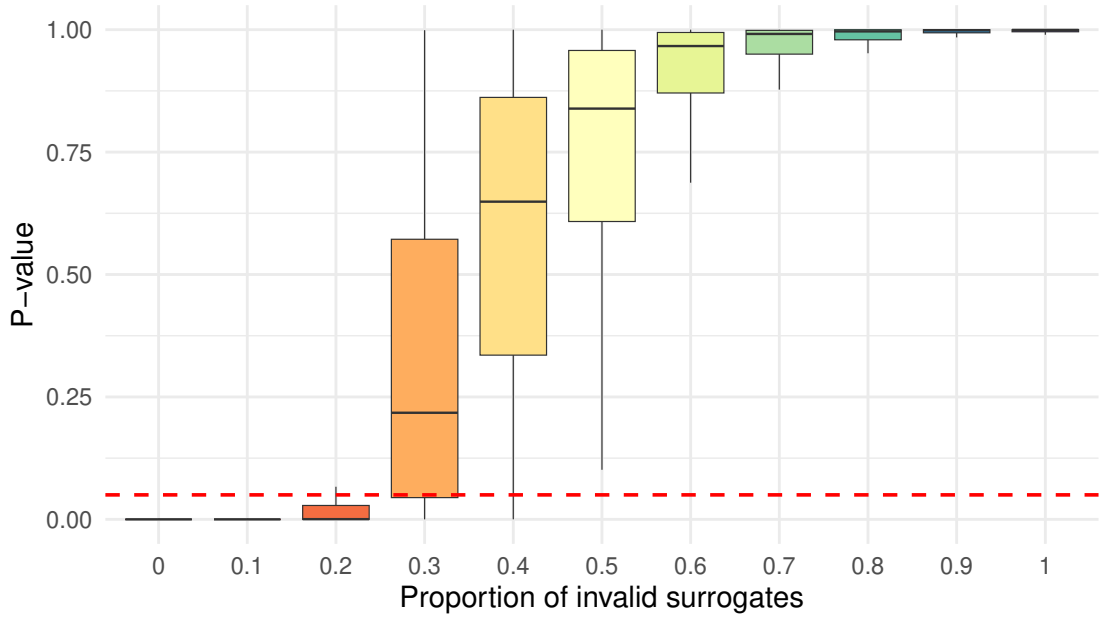

Figure S6: Data generation process 2: The distributions of the p-values in the evaluation step are examined as a function of the false discovery proportion which make up $\widehat{\gamma}_{\mathcal{S}}$, which consists of a combination of 20 predictors. The sample size is $n = 50$ and the valid surrogate strength is $\widehat{U_{S_j}} = 0.9$. The nominal significance level $\alpha = 0.05$ is plotted as a dashed red line. Desired power for the new surrogate was fixed at 80%.

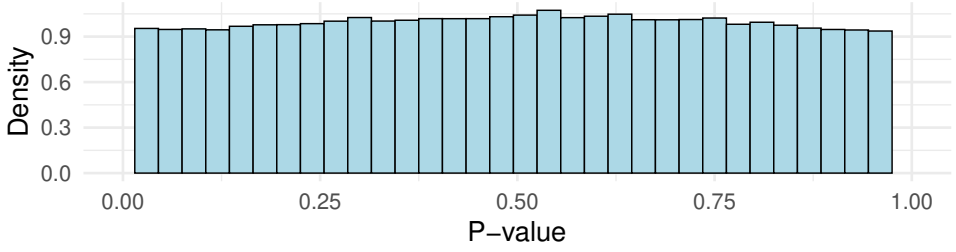

Figure S7: Data generation process 1: distribution of raw p-values under the null hypothesis. The sample size is $n = 50$, the predictors were generated without correlation, and the histogram represents the results across 1000 simulations.

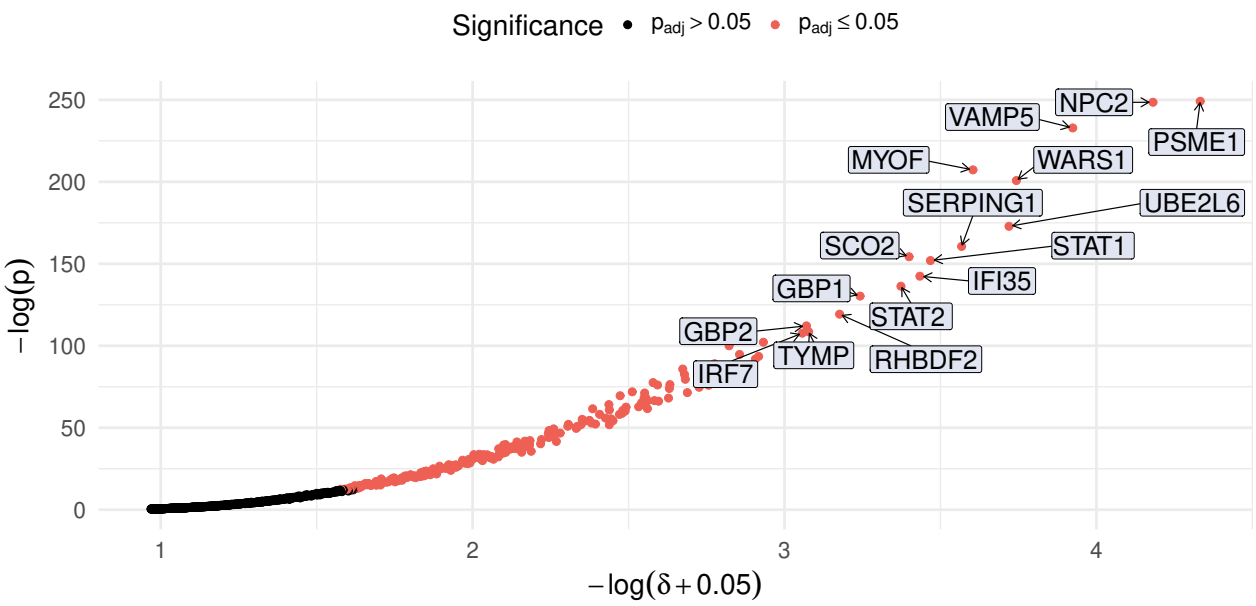

Figure S8: A visual method to select markers to pass the screening stage. The x-axis is the negative log of the δ values, where 0.05 is added to avoid taking the log of 0, and the y-axis is the negative log of the raw p-value. Markers with a stronger surrogate strength appear towards the top-right of the plot. One could select markers without relying on a p-value threshold by choosing those which are most separated from the rest. In this example, the top 16 genes are labelled as they visually separate themselves. Evaluating the combined surrogacy of these genes gives $\delta 95\%\text{C.I.} = -0.01(-1, 0.009)$ corresponding to $p = 2.1e-40$. Points in red are the 235 genes which were selected according to the adjusted p-value threshold of 0.05.

Table S1: Screening results from the data application - all genes with adjusted p-values less than 0.05.

Gene	δ (95% C.I.)	σ_δ	Unadjusted p-value	B-H Adjusted p-value
PSME1	-0.037 (-1, -0.011)	0.016	6.3e-109	6.4e-105
NPC2	-0.035 (-1, -0.009)	0.016	1.2e-108	1.2e-104
VAMP5	-0.03 (-1, -0.004)	0.016	7.3e-102	7.4e-98
MYOF	-0.023 (-1, 0.005)	0.017	9.5e-91	9.6e-87
WARS1	-0.026 (-1, 0.002)	0.017	6.4e-88	6.4e-84
UBE2L6	-0.026 (-1, 0.005)	0.018	8.4e-76	8.4e-72
SERPING1	-0.022 (-1, 0.009)	0.019	1.8e-70	1.8e-66
SCO2	-0.017 (-1, 0.015)	0.019	9.7e-68	9.8e-64
STAT1	-0.019 (-1, 0.013)	0.019	1.0e-66	1.0e-62
IFI35	-0.018 (-1, 0.015)	0.020	1.4e-62	1.4e-58
STAT2	-0.016 (-1, 0.018)	0.020	6.3e-60	6.3e-56
GBP1	-0.011 (-1, 0.023)	0.020	2.6e-57	2.6e-53
RHBDF2	-0.008 (-1, 0.027)	0.021	1.6e-52	1.6e-48
GBP2	-0.004 (-1, 0.032)	0.022	2.0e-49	2.0e-45
TYMP	-0.004 (-1, 0.032)	0.022	7.3e-48	7.4e-44
IRF7	-0.003 (-1, 0.033)	0.022	1.7e-47	1.7e-43
XAF1	0.003 (-1, 0.04)	0.022	4.2e-45	4.3e-41
ADAP2	0.009 (-1, 0.045)	0.022	3.7e-44	3.8e-40
ATF5	0.008 (-1, 0.045)	0.023	7.4e-42	7.4e-38
SP140	0.004 (-1, 0.042)	0.023	2.4e-41	2.5e-37
MAFB	0.005 (-1, 0.043)	0.023	1.3e-40	1.3e-36
P2RY14	0.012 (-1, 0.05)	0.023	2.1e-39	2.1e-35
RBCK1	0.012 (-1, 0.051)	0.023	1.2e-38	1.2e-34
EPB41L3	0.015 (-1, 0.054)	0.023	4.4e-38	4.4e-34
TLR7	0.019 (-1, 0.057)	0.023	5.4e-38	5.5e-34
GCH1	0.015 (-1, 0.054)	0.023	7.8e-38	7.8e-34
OAS1	0.011 (-1, 0.05)	0.024	1.3e-37	1.3e-33
PSMB10	0.011 (-1, 0.05)	0.024	4.1e-37	4.1e-33
ATF3	0.019 (-1, 0.057)	0.023	1.5e-36	1.5e-32
PSTPIP2	0.018 (-1, 0.058)	0.024	2.8e-35	2.8e-31
PSMB9	0.026 (-1, 0.065)	0.024	2.1e-34	2.1e-30
SORT1	0.022 (-1, 0.062)	0.024	7.3e-34	7.4e-30
CNDP2	0.025 (-1, 0.064)	0.024	9.1e-34	9.2e-30
TRAFD1	0.014 (-1, 0.054)	0.025	1.1e-33	1.1e-29
LHFPL2	0.015 (-1, 0.056)	0.025	1.5e-33	1.5e-29
TRIM22	0.015 (-1, 0.057)	0.025	3.6e-33	3.7e-29
SCARB2	0.022 (-1, 0.062)	0.025	7.6e-33	7.7e-29
IFITM3	0.031 (-1, 0.071)	0.024	5.9e-32	5.9e-28
IRF9	0.018 (-1, 0.06)	0.025	9.4e-32	9.5e-28
GADD45B	0.028 (-1, 0.068)	0.025	1.2e-31	1.2e-27
SRBD1	0.034 (-1, 0.074)	0.024	6.4e-31	6.5e-27
IFIH1	0.028 (-1, 0.069)	0.025	2.2e-30	2.2e-26
CEACAM1	0.022 (-1, 0.064)	0.026	2.7e-30	2.7e-26
OAS3	0.028 (-1, 0.069)	0.025	3.2e-30	3.2e-26
DDX58	0.026 (-1, 0.068)	0.026	1.2e-29	1.3e-25
ISG20	0.027 (-1, 0.069)	0.026	1.8e-29	1.8e-25
BST2	0.025 (-1, 0.067)	0.026	1.8e-29	1.8e-25
IFIT3	0.029 (-1, 0.071)	0.026	4.5e-29	4.6e-25
TCN2	0.037 (-1, 0.079)	0.025	1.4e-28	1.4e-24
RTP4	0.028 (-1, 0.071)	0.026	2.0e-28	2.0e-24
MT2A	0.029 (-1, 0.072)	0.026	5.4e-28	5.4e-24
TRIM21	0.033 (-1, 0.075)	0.026	6.7e-28	6.7e-24
SAMD4A	0.027 (-1, 0.071)	0.026	1.6e-27	1.7e-23
SLC6A12	0.042 (-1, 0.083)	0.025	1.8e-27	1.8e-23
ETV7	0.037 (-1, 0.08)	0.026	3.8e-27	3.8e-23
STX11	0.034 (-1, 0.077)	0.026	5.1e-27	5.2e-23
IFI44L	0.033 (-1, 0.076)	0.026	7.6e-27	7.6e-23
OAS2	0.034 (-1, 0.077)	0.027	2.8e-26	2.8e-22
IL15	0.04 (-1, 0.083)	0.026	5.4e-26	5.5e-22
OASL	0.035 (-1, 0.078)	0.027	5.6e-26	5.6e-22
P2RX7	0.038 (-1, 0.083)	0.027	5.4e-25	5.4e-21
DHRS9	0.037 (-1, 0.081)	0.027	8.7e-25	8.7e-21
OGFR	0.045 (-1, 0.089)	0.026	1.2e-24	1.2e-20
IFITM1	0.043 (-1, 0.087)	0.027	2.2e-24	2.2e-20
DENND1A	0.036 (-1, 0.081)	0.027	2.7e-24	2.7e-20
NUCB1	0.044 (-1, 0.088)	0.027	3.2e-24	3.3e-20
HERC5	0.042 (-1, 0.087)	0.027	1.1e-23	1.1e-19
PARP12	0.041 (-1, 0.087)	0.027	2.0e-23	2.0e-19

Gene	δ (95% C.I.)	σ_δ	Unadjusted p-value	Bonferroni Adjusted p-value
PSMB3	0.05 (-1, 0.093)	0.027	2.4e-23	2.5e-19
PLSCR1	0.046 (-1, 0.09)	0.027	2.8e-23	2.8e-19
IRF1	0.037 (-1, 0.083)	0.028	2.9e-23	3.0e-19
SRC	0.05 (-1, 0.094)	0.027	7.7e-23	7.8e-19
CXCL10	0.047 (-1, 0.092)	0.027	9.8e-23	9.9e-19
RSAD2	0.047 (-1, 0.092)	0.027	1.1e-22	1.1e-18
PLEKHO1	0.047 (-1, 0.093)	0.028	2.8e-22	2.8e-18
FAM111A	0.054 (-1, 0.099)	0.027	3.8e-22	3.9e-18
MTMR11	0.056 (-1, 0.101)	0.027	1.0e-21	1.0e-17
TFIP11	0.052 (-1, 0.098)	0.028	5.0e-21	5.0e-17
SQOR	0.056 (-1, 0.102)	0.028	6.9e-21	7.0e-17
TDRD7	0.054 (-1, 0.101)	0.028	3.1e-20	3.1e-16
DHX58	0.056 (-1, 0.103)	0.028	7.3e-20	7.4e-16
MX1	0.059 (-1, 0.106)	0.029	2.6e-19	2.6e-15
DDX60	0.063 (-1, 0.109)	0.028	5.0e-19	5.0e-15
SNTB1	0.064 (-1, 0.111)	0.028	6.8e-19	6.8e-15
TRIM5	0.053 (-1, 0.102)	0.030	8.2e-19	8.3e-15
TNFAIP2	0.067 (-1, 0.114)	0.028	1.1e-18	1.1e-14
MICB	0.063 (-1, 0.11)	0.029	2.5e-18	2.5e-14
IFIT2	0.064 (-1, 0.111)	0.029	2.5e-18	2.6e-14
SP110	0.059 (-1, 0.107)	0.030	3.4e-18	3.4e-14
ATOX1	0.072 (-1, 0.118)	0.028	5.6e-18	5.7e-14
GNS	0.065 (-1, 0.112)	0.029	6.2e-18	6.3e-14
AIM2	0.073 (-1, 0.119)	0.028	7.2e-18	7.2e-14
ADAR	0.063 (-1, 0.111)	0.030	1.1e-17	1.1e-13
ASCL2	0.064 (-1, 0.112)	0.030	1.7e-17	1.7e-13
IFI6	0.069 (-1, 0.116)	0.029	1.9e-17	1.9e-13
AFF1	0.065 (-1, 0.114)	0.030	1.9e-17	1.9e-13
MRPL44	0.07 (-1, 0.117)	0.029	2.4e-17	2.5e-13
MSRB2	0.071 (-1, 0.119)	0.029	3.1e-17	3.1e-13
CALCOCO2	0.066 (-1, 0.115)	0.030	3.7e-17	3.7e-13
SLC2A6	0.069 (-1, 0.117)	0.029	3.9e-17	4.0e-13
LILRB4	0.069 (-1, 0.117)	0.029	4.5e-17	4.6e-13
PLAAT4	0.065 (-1, 0.114)	0.030	4.8e-17	4.9e-13
RIPK2	0.068 (-1, 0.117)	0.030	6.6e-17	6.7e-13
DUSP3	0.074 (-1, 0.122)	0.029	7.1e-17	7.2e-13
HLA_DMB	0.07 (-1, 0.119)	0.030	8.9e-17	8.9e-13
PSMB2	0.073 (-1, 0.121)	0.030	2.2e-16	2.2e-12
TBC1D2B	0.072 (-1, 0.121)	0.030	2.4e-16	2.4e-12
APOL6	0.062 (-1, 0.113)	0.031	3.3e-16	3.3e-12
GSDMD	0.066 (-1, 0.117)	0.031	5.9e-16	5.9e-12
C1QB	0.072 (-1, 0.121)	0.030	6.2e-16	6.2e-12
SLAMF8	0.073 (-1, 0.123)	0.030	1.0e-15	1.0e-11
TNFAIP6	0.083 (-1, 0.131)	0.029	2.0e-15	2.0e-11
KYNU	0.081 (-1, 0.13)	0.030	2.6e-15	2.6e-11
APOL2	0.085 (-1, 0.133)	0.029	2.6e-15	2.6e-11
CYBB	0.079 (-1, 0.129)	0.030	2.8e-15	2.8e-11
PHF11	0.075 (-1, 0.125)	0.031	4.2e-15	4.2e-11
DRAP1	0.078 (-1, 0.128)	0.031	7.1e-15	7.1e-11
IFI44	0.078 (-1, 0.128)	0.031	8.3e-15	8.4e-11
BCAS2	0.083 (-1, 0.133)	0.030	8.9e-15	9.0e-11
TMEM140	0.077 (-1, 0.128)	0.031	9.7e-15	9.8e-11
ACOT9	0.082 (-1, 0.132)	0.030	9.8e-15	9.9e-11
ANKFY1	0.075 (-1, 0.126)	0.031	9.9e-15	1.0e-10
EIF2AK2	0.077 (-1, 0.128)	0.031	1.3e-14	1.3e-10
PLAUR	0.084 (-1, 0.133)	0.030	1.4e-14	1.4e-10
IL12RB1	0.078 (-1, 0.129)	0.031	1.9e-14	1.9e-10
TNF	0.085 (-1, 0.134)	0.030	2.1e-14	2.2e-10
TENT5A	0.082 (-1, 0.133)	0.031	3.8e-14	3.8e-10
DUSP5	0.077 (-1, 0.129)	0.032	4.3e-14	4.3e-10
HLA_DPA1	0.087 (-1, 0.137)	0.030	4.4e-14	4.4e-10
PLAGL2	0.09 (-1, 0.14)	0.030	7.7e-14	7.7e-10
PSMB8	0.081 (-1, 0.133)	0.032	9.7e-14	9.8e-10
PARP3	0.087 (-1, 0.138)	0.031	1.5e-13	1.6e-09
CTRL	0.086 (-1, 0.138)	0.032	3.5e-13	3.5e-09
HLA_DRA	0.09 (-1, 0.141)	0.031	3.7e-13	3.7e-09
RNF114	0.088 (-1, 0.14)	0.032	4.9e-13	5.0e-09
ALDH1A1	0.087 (-1, 0.14)	0.032	5.9e-13	5.9e-09
ETV6	0.096 (-1, 0.147)	0.031	1.2e-12	1.2e-08
FCN1	0.093 (-1, 0.145)	0.032	1.3e-12	1.3e-08
LAMP3	0.095 (-1, 0.147)	0.031	1.7e-12	1.8e-08

Gene	δ (95% C.I.)	σ_δ	Unadjusted p-value	Bonferroni Adjusted p-value
TOR1B	0.093 (-1, 0.145)	0.032	2.3e-12	2.3e-08
CDC42EP2	0.092 (-1, 0.145)	0.032	2.6e-12	2.7e-08
MICU1	0.101 (-1, 0.151)	0.031	3.0e-12	3.0e-08
IFI16	0.093 (-1, 0.146)	0.033	5.7e-12	5.7e-08
TAPBP	0.096 (-1, 0.148)	0.032	5.9e-12	5.9e-08
AKR1A1	0.095 (-1, 0.148)	0.032	6.0e-12	6.0e-08
IFIT5	0.098 (-1, 0.15)	0.032	8.4e-12	8.4e-08
DMXL2	0.098 (-1, 0.151)	0.032	1.1e-11	1.1e-07
DRAM1	0.104 (-1, 0.156)	0.032	1.4e-11	1.4e-07
LGALS3BP	0.1 (-1, 0.153)	0.032	1.5e-11	1.5e-07
MX2	0.101 (-1, 0.153)	0.032	1.6e-11	1.6e-07
SOCS1	0.096 (-1, 0.15)	0.033	2.1e-11	2.1e-07
SLC27A3	0.095 (-1, 0.15)	0.034	3.7e-11	3.7e-07
KREMEN2	0.107 (-1, 0.16)	0.032	5.6e-11	5.7e-07
GAS6	0.108 (-1, 0.161)	0.032	8.0e-11	8.0e-07
CUL1	0.103 (-1, 0.157)	0.033	9.8e-11	9.9e-07
UNC93B1	0.105 (-1, 0.159)	0.033	1.4e-10	1.4e-06
ARSB	0.109 (-1, 0.162)	0.032	1.4e-10	1.4e-06
CARS2	0.11 (-1, 0.163)	0.032	1.7e-10	1.7e-06
IRF2	0.109 (-1, 0.163)	0.033	2.5e-10	2.5e-06
REC8	0.102 (-1, 0.158)	0.034	3.3e-10	3.3e-06
BLVRA	0.108 (-1, 0.163)	0.033	4.2e-10	4.3e-06
VAMP3	0.115 (-1, 0.169)	0.033	5.4e-10	5.4e-06
TIMM10	0.105 (-1, 0.161)	0.034	5.4e-10	5.5e-06
HEBP1	0.107 (-1, 0.163)	0.034	6.8e-10	6.8e-06
NFKBIE	0.113 (-1, 0.168)	0.033	1.0e-09	1.0e-05
TAPBPL	0.11 (-1, 0.166)	0.034	1.0e-09	1.0e-05
CIITA	0.108 (-1, 0.165)	0.034	1.1e-09	1.1e-05
SPATS2L	0.117 (-1, 0.171)	0.033	1.1e-09	1.1e-05
PANK2	0.118 (-1, 0.172)	0.033	1.1e-09	1.1e-05
GSTK1	0.112 (-1, 0.168)	0.034	1.4e-09	1.4e-05
LY6E	0.11 (-1, 0.167)	0.034	1.6e-09	1.7e-05
CTSL	0.117 (-1, 0.172)	0.033	1.9e-09	1.9e-05
PML	0.114 (-1, 0.17)	0.034	1.9e-09	1.9e-05
IFIT1	0.117 (-1, 0.172)	0.034	2.8e-09	2.8e-05
HLA_DMA	0.112 (-1, 0.17)	0.035	3.3e-09	3.3e-05
ATP1B3	0.12 (-1, 0.175)	0.034	3.8e-09	3.8e-05
EIF4E2	0.124 (-1, 0.178)	0.033	4.0e-09	4.0e-05
APOBEC3G	0.125 (-1, 0.179)	0.033	4.1e-09	4.2e-05
APOBEC3F	0.124 (-1, 0.178)	0.033	5.4e-09	5.4e-05
PLEK	0.124 (-1, 0.179)	0.033	6.4e-09	6.4e-05
PSENEN	0.131 (-1, 0.184)	0.032	6.8e-09	6.8e-05
ILK	0.125 (-1, 0.18)	0.033	8.0e-09	8.1e-05
KARS1	0.125 (-1, 0.18)	0.033	8.8e-09	8.9e-05
TNFSF10	0.125 (-1, 0.181)	0.034	1.2e-08	1.2e-04
TICAM1	0.126 (-1, 0.182)	0.034	1.4e-08	1.4e-04
KCNMB1	0.12 (-1, 0.177)	0.035	1.6e-08	1.6e-04
CD300A	0.122 (-1, 0.179)	0.035	1.8e-08	1.9e-04
CASP5	0.13 (-1, 0.186)	0.034	2.7e-08	2.8e-04
DECR1	0.134 (-1, 0.189)	0.033	3.2e-08	3.2e-04
SELL	0.132 (-1, 0.188)	0.034	4.0e-08	4.0e-04
RERE	0.127 (-1, 0.184)	0.035	4.0e-08	4.1e-04
FIG4	0.124 (-1, 0.182)	0.035	4.2e-08	4.2e-04
PEA15	0.128 (-1, 0.185)	0.035	4.9e-08	4.9e-04
TM9SF1	0.13 (-1, 0.187)	0.035	5.4e-08	5.5e-04
KCNJ2	0.132 (-1, 0.189)	0.035	7.5e-08	7.5e-04
RELB	0.141 (-1, 0.196)	0.033	1.1e-07	1.1e-03
PSMA5	0.139 (-1, 0.195)	0.034	1.2e-07	1.2e-03
CD300C	0.139 (-1, 0.195)	0.034	1.2e-07	1.3e-03
NAGK	0.135 (-1, 0.192)	0.035	1.4e-07	1.4e-03
CASZ1	0.133 (-1, 0.191)	0.035	1.4e-07	1.4e-03
AGPAT3	0.139 (-1, 0.195)	0.034	1.7e-07	1.7e-03
PDK3	0.138 (-1, 0.195)	0.035	1.9e-07	1.9e-03
NOD2	0.14 (-1, 0.196)	0.034	2.1e-07	2.2e-03
BTN3A3	0.133 (-1, 0.192)	0.036	2.2e-07	2.2e-03
CASP1	0.14 (-1, 0.197)	0.035	2.5e-07	2.5e-03
SECTM1	0.142 (-1, 0.198)	0.034	2.6e-07	2.6e-03
ELF4	0.132 (-1, 0.192)	0.036	2.8e-07	2.9e-03
TRIM26	0.134 (-1, 0.194)	0.036	3.2e-07	3.2e-03
MARCO	0.138 (-1, 0.196)	0.035	3.4e-07	3.4e-03
DHDDS	0.138 (-1, 0.196)	0.036	3.6e-07	3.6e-03

Gene	δ (95% C.I.)	σ_δ	Unadjusted p-value	Bonferroni Adjusted p-value
PSEN2	0.145 (-1, 0.201)	0.034	3.9e-07	3.9e-03
LMO2	0.147 (-1, 0.203)	0.034	4.3e-07	4.3e-03
FGL2	0.145 (-1, 0.202)	0.035	5.4e-07	5.5e-03
BTN3A1	0.143 (-1, 0.201)	0.035	5.5e-07	5.5e-03
CD40	0.143 (-1, 0.201)	0.035	6.0e-07	6.0e-03
TYROBP	0.148 (-1, 0.205)	0.035	1.0e-06	1.0e-02
ALDH2	0.147 (-1, 0.205)	0.035	1.1e-06	1.1e-02
TNS3	0.146 (-1, 0.204)	0.036	1.1e-06	1.1e-02
SP100	0.144 (-1, 0.204)	0.036	1.3e-06	1.4e-02
SLC7A7	0.15 (-1, 0.207)	0.035	1.4e-06	1.4e-02
SMARCD3	0.147 (-1, 0.205)	0.036	1.5e-06	1.5e-02
DPYSL2	0.148 (-1, 0.207)	0.036	1.7e-06	1.7e-02
NFKBIB	0.145 (-1, 0.205)	0.036	1.7e-06	1.7e-02
TMEM51	0.151 (-1, 0.209)	0.035	1.9e-06	1.9e-02
SLC25A22	0.146 (-1, 0.205)	0.036	1.9e-06	1.9e-02
SLC20A1	0.151 (-1, 0.209)	0.035	1.9e-06	2.0e-02
GSTO1	0.149 (-1, 0.208)	0.036	2.2e-06	2.2e-02
EMILIN2	0.154 (-1, 0.212)	0.036	3.6e-06	3.6e-02
CTSS	0.152 (-1, 0.212)	0.036	3.9e-06	3.9e-02
ANXA5	0.153 (-1, 0.212)	0.036	4.0e-06	4.1e-02
ASGR1	0.156 (-1, 0.214)	0.035	4.1e-06	4.1e-02
FAR2	0.157 (-1, 0.214)	0.035	4.1e-06	4.2e-02
GNA15	0.148 (-1, 0.209)	0.037	4.3e-06	4.3e-02
FFAR2	0.15 (-1, 0.211)	0.037	4.4e-06	4.5e-02
SHTN1	0.154 (-1, 0.213)	0.036	4.5e-06	4.5e-02

Table S2: Sensitivity analysis evaluating the effect of varying the non-inferiority margin ϵ, where values closer to 0 result in fewer candidate surrogates to combine for the evaluation stage. The evaluation metric for the combined marker, $\boldsymbol{\delta}_{\boldsymbol{\gamma_S}}$, its standard deviation, and its p-value corresponding to a test based on a desired power of 90% are given in the table.

ϵ (screening)	No. of genes in γ_S	δ_{γ_S} (95% C.I.)	$\sigma_{\delta_{\gamma_S}}$	p-value
0.05	4	-0.01 (-1, 0.009)	0.012	2.1e-40
0.10	16	-0.01 (-1, 0.009)	0.012	2.1e-40
0.15	55	-0.006 (-1, 0.015)	0.013	2.0e-32
0.20	104	-0.006 (-1, 0.015)	0.013	2.0e-32
0.25	154	-0.006 (-1, 0.015)	0.013	2.0e-32
0.30	215	-0.006 (-1, 0.015)	0.013	2.0e-32
0.35	302	-0.006 (-1, 0.015)	0.013	2.0e-32